



Efficient photocatalytic degradation of thiobencarb over BiVO₄ driven by visible light: Parameter and reaction pathway investigations



Hsiao-Fang Lai^a, Chiing-Chang Chen^b, Yi-Kuo Chang^c, Chung-Shin Lu^{d,*}, Ren-Jang Wu^{a,*}

^a Department of Applied Chemistry, Providence University, Taichung 433, Taiwan, ROC

^b Department of Science Application and Dissemination, National Taichung University of Education, Taichung 403, Taiwan, ROC

^c Department of Safety Health and Environmental Engineering, Central Taiwan University of Science and Technology, Taichung 406, Taiwan, ROC

^d Department of General Education, National Taichung University of Science and Technology, Taichung 403, Taiwan, ROC

ARTICLE INFO

Article history:

Received 23 February 2013

Received in revised form 29 October 2013

Accepted 30 October 2013

Available online 9 November 2013

Keywords:

Photocatalysis

Visible light

BiVO₄

Thiobencarb

Pathway

ABSTRACT

In this study, BiVO₄ powder with monoclinic structure was prepared and used as a visible-light catalyst for the photocatalytic degradation of thiobencarb (TBC). To the best of our knowledge, this is the first time reporting the photocatalytic degradation of TBC using BiVO₄ as the catalyst. The as-prepared BiVO₄ photocatalyst was characterized by X-ray diffraction (XRD), scanning electron microscopy (SEM), X-ray photoelectron spectroscopy (XPS) and UV–vis diffuse reflectance spectra (DRS). With the presence of both H₂O₂ and BiVO₄ catalysts, TBC could be effectively degraded under visible-light irradiation. The degradation efficiency of TBC was 97% after 5 h in the photocatalytic process. Factors such as catalyst dosage, solution pH, hydrogen peroxide concentration and the presence of anions were found to influence the degradation rate. The BiVO₄ powder displayed a good stability and maintained a high photocatalytic performance during three successive runs. To scrutinize the mechanistic details of the TBC photodegradation, the intermediates of the process were separated, identified, and characterized by solid-phase microextraction (SPME) and gas chromatography/mass spectrometry (GC/MS) technique. The probable photodegradation pathways were proposed and discussed. The results would provide useful information for the research of thiocarbamate decomposition and the development of new applications of BiVO₄.

© 2013 Elsevier B.V. All rights reserved.

1. Introduction

Thiobencarb (TBC, S-4-chlorobenzyl diethylthiocarbamate) is a thiocarbamate herbicide that has been commonly used in rice fields, at a worldwide (40 countries) rate of approximately 18,000 tons per year [1]. It may contaminate the environment through constant leaching and superficial runoff during rainfall. TBC is resistant to degradation by hydrolysis and has been detected in river waters. It is moderately toxic to aquatic invertebrates and fish in acute toxicity tests [2,3]. The US Environmental Protection Agency (USEPA) researchers have reported the reference dose 0.01 mg/kg/d TBC in publicly accessible databases, such as the Integrated Risk Information System. The Ministry of the Environment in Japan released the Environmental Quality Standards for Water Pollutants being 0.02 mg L⁻¹ of TBC [4]. Because TBC can cause some environmental problems, the development of a simple and effective removal method is necessary.

Various methods have been reported to remove organic compound from polluted water, such as physical adsorption

[5,6], biological method [7–9], chemical oxidation [10,11] and photocatalytic method [12,13]. Among these methods, photocatalytic degradation is promising due to its high degradation and mineralization efficiency. As the most widely studied material in the field of photocatalysis, TiO₂ has been used for degrading TBC successfully [14,15]. However, the main shortcoming of TiO₂ is that it only absorbs ultraviolet light less than 387.5 nm, which only accounts for about 4% of sunlight. High energy is necessary to keep its degradation efficiency when TiO₂ is used for treating organic chemicals in water [16–18]. Therefore, it is very important to develop the visible-light-sensitive photocatalyst, which can efficiently utilize the inexpensive and inexhaustible solar energy.

In recent years, BiVO₄ has been demonstrated to be a good visible-light-driven photocatalyst [19–21]. It possesses a bandgap of 2.3–2.4 eV, which is smaller than that of the TiO₂ photocatalyst (3.2 eV) and shows well absorption for visible light [22]. It is well known that BiVO₄ mainly possesses three crystal forms, tetragonal zircon structure, monoclinic scheelite structure and tetragonal scheelite structure. Among these crystalline structures, only monoclinic BiVO₄ shows a well response to visible light [23]. It was reported that some organic substances could be degraded in such a monoclinic BiVO₄ suspension system under visible-light irradiation [24–27].

* Corresponding authors. Tel.: +886 4 2219 6999; fax: +886 4 2219 6825 (C.S. Lu), tel.: +886 4 2632 8001; fax: +886 4 2632 7554 (R.J. Wu).

E-mail addresses: cslu6@nutc.edu.tw (C.-S. Lu), rjwu@pu.edu.tw (R.-J. Wu).

To the best of our knowledge, no prior study has investigated the degradation of thiocarbamate herbicides by visible-light-driven photocatalyst and that very little is known about the use of BiVO_4 in the treatment of thiocarbamates in aqueous solution. In this paper, we report the photocatalytic degradation of thiobencarb using BiVO_4 as catalyst for the first time. We investigate various parameters that may affect the photodegradation of TBC in the presence of BiVO_4 suspensions in order to obtain a better understanding on BiVO_4 photocatalysis. This study also focuses on the identification of the reaction intermediates and the understanding of mechanistic details of the photodegradation of TBC in the BiVO_4 /visible light process.

2. Experimental

2.1. Material

Thiobencarb was obtained from Sigma–Aldrich (99.8%) and used without further purification. Stock solution containing 5 mg L^{-1} of TBC in water was prepared, protected from light, and stored at 4°C . HPLC analysis was employed to confirm the presence of TBC as a pure organic compound. Bismuth nitrate $\text{Bi}(\text{NO}_3)_3 \cdot 5\text{H}_2\text{O}$ (Aldrich, 98%) and ammonium metavanadate NH_4VO_3 (Panreac, 99%) were used as the precursors of bismuth vanadate (BiVO_4). Reagent-grade ammonium acetate, sodium hydroxide, nitric acid, and HPLC-grade methanol were purchased from Merck. De-ionized water was used throughout this study. The water was purified with a Milli-Q water ion-exchange system (Millipore Co.) to give a resistivity of $1.8 \times 10^7 \Omega \text{ cm}$.

2.2. Preparation and characterization of BiVO_4

Forty mmole of $\text{Bi}(\text{NO}_3)_3 \cdot 5\text{H}_2\text{O}$ and 40 mmol of NH_4VO_3 were dissolved separately into 500 mL of 2.0 mol L^{-1} nitric acid solution. After the solutions of $\text{Bi}(\text{NO}_3)_3 \cdot 5\text{H}_2\text{O}$ and NH_4VO_3 being mixed with each other, 7.5 g of urea was added. Then the mixed solution was stirred for 24 h at 90°C . The vivid yellow precipitate was washed with distilled water and absolute alcohol for several times, and then dried at 60°C for 10 h. Finally, the dried powder was calcined at 450°C for 15 min.

The phase and composition of the as-prepared BiVO_4 powder were measured by X-ray diffraction (XRD) using an X-ray diffractometer (PHILIPS X'PERT Pro MPD). The morphology of the BiVO_4 powder was analyzed using a field-emission scanning electron microscope (FE-SEM, HITACHI S-4800). The binding energy of Bi, V, and O was measured at room temperature using an X-ray photoelectron spectroscope (XPS, VG Scientific ESCALAB 250). The peak position of each element was corrected by C1s (284.6 eV). UV–vis diffuse reflectance spectrum of the BiVO_4 powder was measured using a UV–vis spectrophotometer equipped with an integration sphere (Perkin Elmer Lambda 35).

2.3. Apparatus and instruments

The apparatus for studying the photocatalytic degradation of TBC has been described elsewhere [28]. The C-75 Chromato-Vue cabinet of UVP provides a wide area of illumination from the 15-W visible-light tubes positioned on two sides of the cabinet interior. A Waters LC system, equipped with a binary pump, an autosampler, and a photodiode array detector, was used for determining the amount of TBC in the aqueous solution. Solid-phase microextraction (SPME) and gas chromatography/mass spectrometry (GC/MS) were utilized for the analysis of intermediate products resulted from the photocatalytic degradation process. SPME holder and fiber-coating divinylbenzene-carboxen-polydimethylsiloxane

(DVB-CAR-PDMS 50/30 μm) were supplied from Supelco (Bellefonte, PA). GC/MS analyses were run on a Perkin-Elmer AutoSystem-XL gas chromatograph interfaced to a TurboMass selective mass detector.

2.4. Procedures and analysis

TBC solution (5 mg L^{-1}) with the appropriate amount of photocatalyst was mixed and used in photocatalytic experiments. For reactions in different pH media, the initial pH of the suspension was adjusted by adding either NaOH or HNO_3 solution. Prior to irradiation, the suspension was magnetically stirred in the dark for ca. 30 min to ensure the establishment of the adsorption/desorption equilibrium. Then the appropriate amount of hydrogen peroxide was added. Irradiation was carried out using two visible lamps (15 W). The lamp mainly provides visible light in the range of 400–700 nm. The average light intensity striking the surface of the reaction solution was about 1420 lux, as measured by a digital luxmeter. At any given irradiation time interval, the suspension was sampled (5 mL) and centrifuged to separate the BiVO_4 powders. After each irradiation cycle, the amount of the TBC residual was thus determined by HPLC. Two different kinds of solvents were prepared in this study. Solvent A was 25 mM aqueous ammonium acetate buffer (pH 6.9), while solvent B was methanol. LC was carried out on an Atlantis™ dC18 column (250 mm \times 4.6 mm i.d., $\text{dp} = 5 \mu\text{m}$). The flow rate of the mobile phase was set at 1 mL/min. A linear gradient was run as follows, $t = 0$, $A = 95$, $B = 5$; $t = 20$, $A = 50$, $B = 50$; $t = 35$ – 40 , $A = 10$, $B = 90$; and, $t = 45$, $A = 95$, $B = 5$. The elution was monitored at 220 nm.

The analyses of organic intermediates were accomplished by SPME-GC/MS. The SPME fiber was directly immersed into the sample solution to extract TBC and its intermediates for 30 min at room temperature, with magnetic stirring at $550 \pm 10 \text{ rpm}$ on the Corning stirrer/plate (Corning, USA). Finally, the compounds were thermally desorbed from the fiber to the GC injector for 45 min. Separation was carried out in a DB-5 capillary column (5% diphenyl/95% dimethyl-siloxane), 60 m, 0.25-mm i.d., and 1.0- μm thick film. A split-splitless injector was used under the conditions of injector temperature 250°C and split flow 10 mL/min. The helium carrier gas flow was 1.5 mL/min. The oven temperature was programmed at 60°C for 1.0 min then increased at 8°C min^{-1} until reaching 240°C . It was kept at this temperature for 21.5 min, and the total run time was 45 min.

Mass spectrometric detection was performed in full-scan conditions for both electron impact (EI) and chemical ionization (CI) using isobutane as the reagent gas. The ion source and inlet line temperatures were set at 220 and 250°C , respectively. Electron impact mass spectra were obtained at 70 eV of electron energy and monitored from 20 to 350 m/z . The mass spectrometer was tuned regularly with perfluorotributylamine using the fragment ions at m/z 69, 131, 219 and 502. EI mass spectra were identified using the NIST 2008 Library, and the analytes were automatically identified by the NIST MS-Search 2.0 software. Chemical ionization mass spectrometry was operated in the positive ionization mode, and isobutane was used as the reagent gas at an apparent pressure of 4.4×10^{-4} Torr in the ionization source. The full scan mode with a mass range of m/z 40–350 was used for confirming the analytes. The autotuning software performed the reagent gas flow adjustment and the lens and electronic tuning.

2.5. Analysis of hydroxyl radicals

The formation of hydroxyl radicals ($\cdot\text{OH}$) in the $\text{Vis/BiVO}_4/\text{H}_2\text{O}_2$ system was detected by the fluorescence technique using coumarin as a probe molecule. The experimental procedures were similar to those used in the measurement of photocatalytic activity except

that the aqueous solution of TBC was replaced by an aqueous solution of 1×10^{-3} M coumarin. The visible light irradiation was continuous and sampling was performed every 2 h for analysis. The solution was analyzed after filtration on a Shimadzu RF-5301PC fluorescence spectrophotometer. The product of the coumarin hydroxylation, 7-hydroxycoumarin, gave a peak at a wavelength of about 456 nm by excitation with a wavelength of 332 nm.

3. Results and discussion

3.1. Characterization of BiVO_4

The phase and composition of the as-prepared BiVO_4 were characterized by XRD, as shown in Fig. 1. All the diffraction peaks can be well indexed to a pure monoclinic scheelite phase BiVO_4 of lattice constants $a = 5.197 \text{ \AA}$, $b = 11.704 \text{ \AA}$ and $c = 5.092 \text{ \AA}$, which agrees with the reported values of $a = 5.195 \text{ \AA}$, $b = 11.701 \text{ \AA}$ and $c = 5.092 \text{ \AA}$ (JCPDS No. 14-0688). The main peaks can be indexed as (110), (011), (121), (040), (200), (002), (211), (150), (132), (240), (042), (202), (161), (321) and (123) planes of monoclinic BiVO_4 .

Fig. 2 shows the morphology of the synthesized BiVO_4 powder under a field-emission SEM microscope. The SEM analysis indicated that the microparticles of the BiVO_4 sample were mainly polyhedral in morphology (6–8 μm in edge length), but a small amount of irregular particles was also formed in BiVO_4 . EDS analysis revealed percent content of the elements (wt.%) as Bi, 61.65%; V, 15.05%; O, 18.24%, indicating that the elemental composition of the as-prepared product consisted of bismuth, vanadium, and oxygen with a molar ratio of $\text{Bi}:\text{V}:\text{O} = 13.71:13.73:52.99$, which was very close to the $\text{Bi}:\text{V}$ molar ratio (1:1) in monoclinic BiVO_4 .

The optical absorption property of a semiconductor, relevant to the electronic structure feature, was recognized as the key factor in determining its photocatalytic activity [29]. The UV–vis diffuse reflectance spectrum of the as-prepared BiVO_4 is shown in Fig. 3. According to the spectrum, the BiVO_4 powder presented the photo-absorption properties from the UV light region to visible-light region until 550 nm. The band gap (E_g) of BiVO_4 was estimated to be 2.35 eV, indicating that the BiVO_4 sample had a band gap suitable for photocatalytic degradation of organic contaminants under visible-light irradiation [30].

The XPS spectra of the as-prepared BiVO_4 exhibited the characteristic spin–orbit split of $\text{Bi}4f_{5/2}$ and $\text{Bi}4f_{7/2}$ signals, $\text{V}2p_{1/2}$ and $\text{V}2p_{3/2}$ signals, and $\text{O}1s$ peak (Fig. 4). The $\text{Bi}4f$ orbital showed splitting peaks at 159.1 and 164.3 eV, and the $\text{V}2p$ orbital showed the peaks at 517.2 and 524.6 eV. The observed $\text{O}1s$ peak at 530.2 eV could be assigned to the lattice oxygen in crystalline BiVO_4 [31].

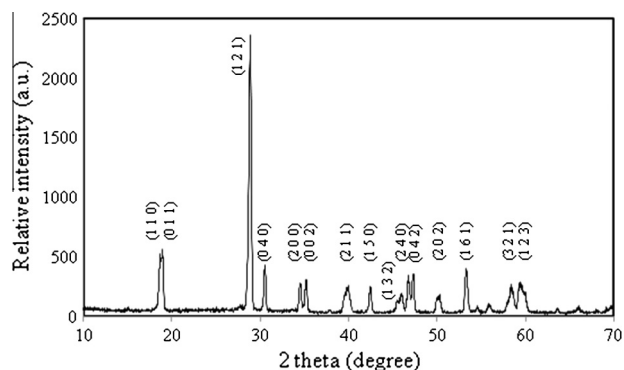
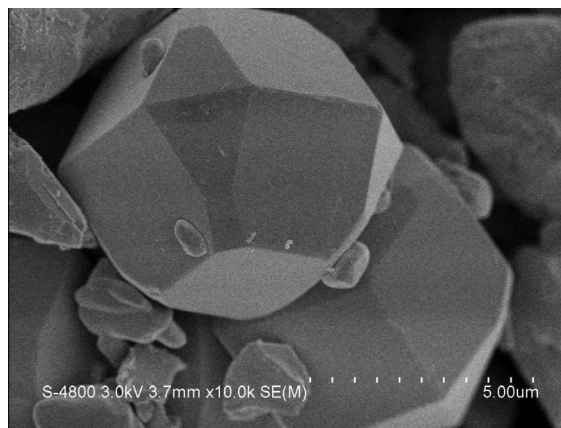
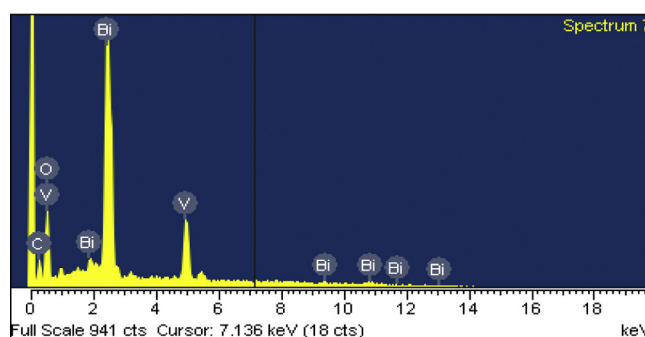


Fig. 1. XRD pattern of the as-prepared BiVO_4 photocatalyst.



(a)



(b)

Fig. 2. SEM image and EDS spectrum of the as-prepared BiVO_4 photocatalyst.

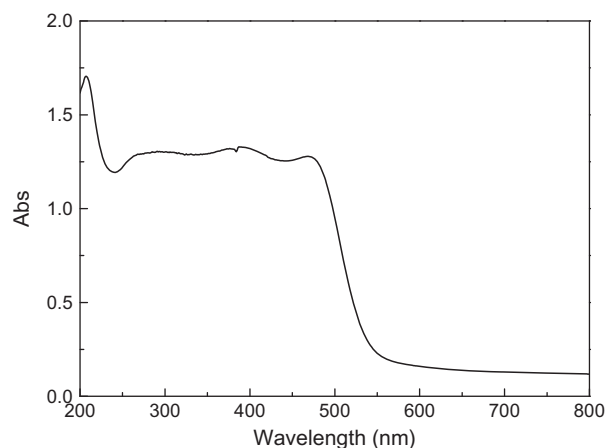


Fig. 3. UV–vis diffuse reflectance spectrum of the as-prepared BiVO_4 photocatalyst.

3.2. Photocatalytic reaction

3.2.1. Effect of H_2O_2 dosage on the degradation of TBC

Fig. 5 shows the photodegradation efficiencies of TBC as a function of irradiation time with the as-prepared BiVO_4 and different amount of H_2O_2 under visible-light irradiation. The results indicated that if only the BiVO_4 powder was added in the solution under visible-light irradiation, TBC did not show photodegradation. However, the degradation rate increased significantly when a small amount of H_2O_2 was added. The degradation rate increased from 12% to 54% as a consequence of increasing H_2O_2 dosage from 8.75 to 17.5 mg L^{-1} after 3 h irradiation. The possible photocata-

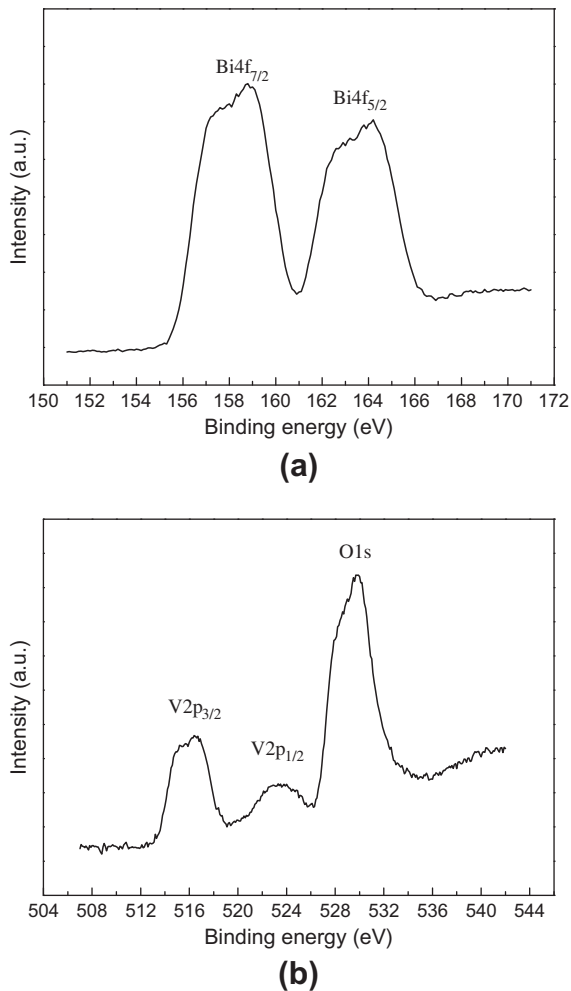


Fig. 4. XPS spectra of the as-prepared BiVO_4 photocatalyst: (a) Bi 4f and (b) V 2p and O 1s.

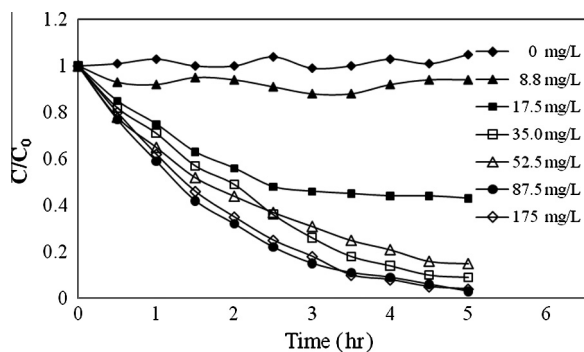
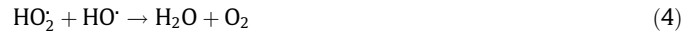


Fig. 5. Effect of H_2O_2 dosage on the photocatalytic degradation rate of TBC. Experimental conditions: TBC concentration 5 mg L^{-1} ; BiVO_4 concentration 1 g L^{-1} ; pH 6.0.

lytic mechanism in the $\text{Vis}/\text{BiVO}_4/\text{H}_2\text{O}_2$ system was described as follows [30].



The generation of photogenerated electron and hole occurred when the BiVO_4 suspension irradiated under visible light (Eq. (1)). Hydrogen peroxide was one of the most effective electron-trapping agents, and HO^\cdot was generated when H_2O_2 trapped the photogenerated electron (Eq. (2)). The HO^\cdot generated from the above reaction had strong oxidizing ability and was available to oxidize TBC. Therefore, the appropriate amount of added hydrogen peroxide could enhance the photocatalytic degradation efficiency.

Nevertheless, it was observed that there was an optimum dosage for H_2O_2 ; either too high or too low dosage could decrease the degradation efficiency. The highest degradation efficiency was observed on the system with 87.5 mg L^{-1} H_2O_2 , which could degrade 97% of TBC in 5 h. When the amount of H_2O_2 was insufficient, there was not enough HO^\cdot generated acting as the oxidizer, thus leading to a weaker photocatalytic activity. On the other hand, when H_2O_2 was overdosed, the photocatalytic activity also decreased because of the presence of excess H_2O_2 . The excess H_2O_2 molecules scavenged the valuable HO^\cdot and generated a much weaker hydroxyl radical HO_2^\cdot (Eq. (3)), which generally did not play an important role in the oxidation process due to their lower reactivity compared to HO^\cdot radicals [32]. As shown in Eq. (4), the HO_2^\cdot radicals could further react with the remaining HO^\cdot to form ineffective oxygen and water. In addition, the excess H_2O_2 molecules could react with oxidative h^+ on the catalyst surface (Eq. (5)), generating a much weaker oxidizer, O_2 , and the overall oxidation capabilities of the system were dramatically reduced [33].

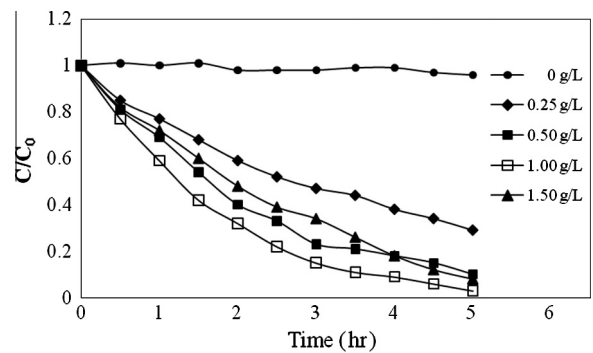


Fig. 6. Effect of BiVO_4 dosage on the photocatalytic degradation rate of TBC. Experimental conditions: TBC concentration 5 mg L^{-1} ; H_2O_2 concentration 87.5 mg L^{-1} ; pH 6.0.

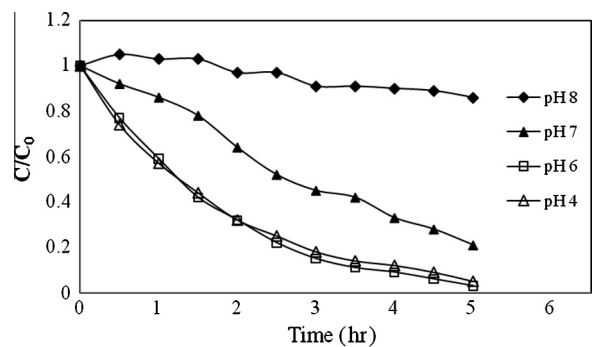


Fig. 7. pH effect on the photocatalytic degradation rate of TBC. Experimental conditions: TBC concentration 5 mg L^{-1} ; BiVO_4 concentration 1 g L^{-1} ; H_2O_2 concentration 87.5 mg L^{-1} .

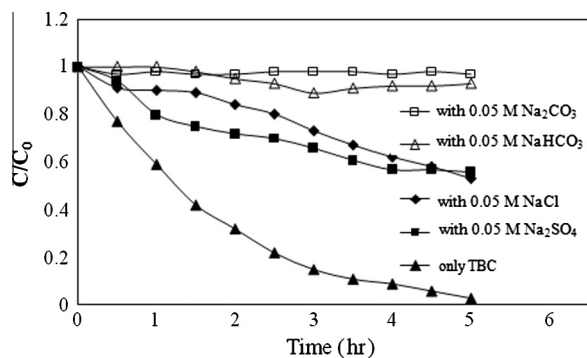


Fig. 8. Effect of anions on the photocatalytic degradation rate of TBC. Experimental conditions: TBC concentration 5 mg L^{-1} ; BiVO_4 concentration 1 g L^{-1} ; H_2O_2 concentration 87.5 mg L^{-1} ; pH 6.0.

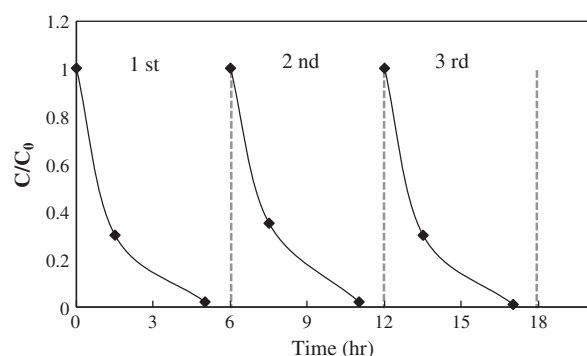


Fig. 9. Cycling runs in the photocatalytic degradation of TBC in the presence of H_2O_2 and BiVO_4 catalyst under visible-light irradiation.

3.2.2. Effect of catalyst dosage on the degradation of TBC

In photocatalytic processes, the amount of photocatalyst was an important parameter to affect the degradation rate of organic com-

pounds. Hence, the effect of BiVO_4 dosage on the photodegradation rate of TBC was investigated by employing different concentration of BiVO_4 varying from 0.25 to 1.5 g L^{-1} . The results clearly showed that degradation under visible-light irradiation without catalysts for 5 h was negligibly small, compared with the results obtained in the presence of BiVO_4 photocatalysts with different dosages (Fig. 6). The photocatalytic degradation rate was found to increase with increasing BiVO_4 dosages, but the reaction was retarded at high BiVO_4 dosages. The increase in the rate was likely due to the increase in the total surface area (or number of active sites) available for photocatalytic reaction as the dosage of BiVO_4 increased. However, when BiVO_4 was overdosed, the intensity of incident visible light was attenuated because of the decreased light penetration and the increased light scattering, which counteracted the positive effect coming from the dosage increment and therefore reduced the overall performance [34,35].

3.2.3. Effect of initial pH value on the degradation of TBC

The influence of the initial pH value on the photodegradation rate of TBC in the $\text{Vis/BiVO}_4/\text{H}_2\text{O}_2$ system is shown in Fig. 7. The dosage of BiVO_4 and H_2O_2 were fixed at 1.0 g L^{-1} and 87.5 mg L^{-1} , respectively. The results indicated that the degradation rate decreased with an increase in pH, and it proceeded much faster under an acidic pH. The reason for lower performance of the $\text{Vis/BiVO}_4/\text{H}_2\text{O}_2$ at higher pH levels was likely because of the special property of H_2O_2 [33,36]. In alkaline medium, H_2O_2 became highly unstable and self-decomposition of H_2O_2 occurred, which was strongly dependent on pH [37]. The self-decomposition would rapidly break down the H_2O_2 molecules into water and oxygen (see Eq. (6)) and make the molecule lose its characteristics as oxidant and most importantly the source of hydroxyl radicals.



Therefore, the degradation rate of TBC in $\text{Vis/BiVO}_4/\text{H}_2\text{O}_2$ process was significantly reduced at higher pH value. Because H_2O_2 could significantly enhance TBC degradation efficiency, it was reasonable to carry out the process in a favorable and relatively mild condition.

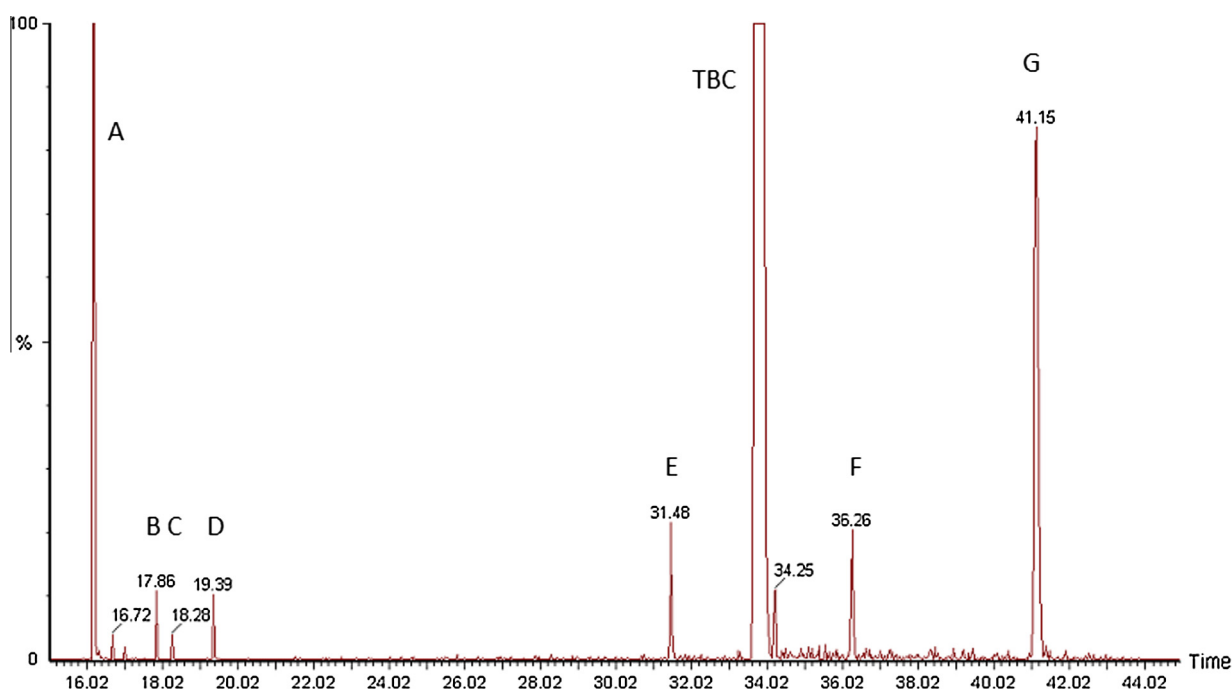
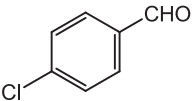
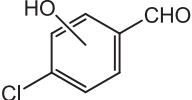
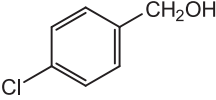
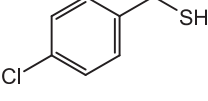
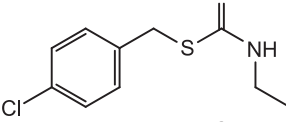
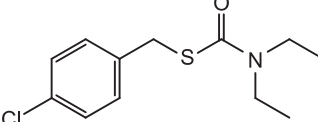
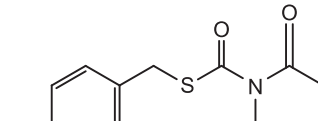
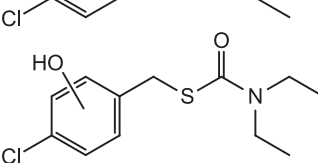


Fig. 10. GC/MS chromatogram obtained for TBC solution (100 mg L^{-1}) after 14 h of irradiation with visible light in the presence of BiVO_4 (1 g L^{-1}) and H_2O_2 (87.5 mg L^{-1}).

Table 1
Identification of the intermediates from the photodegradation of thiobencarb by GC/MS.

Structure	t_R (min)	Characteristic ions (m/z)
	16.21	$[M]^+$ = 140,139,111,75,50 (A) 4-chlorobenzaldehyde
	17.86	$[M]^+$ = 156,155,99,63,39 (B) 4-chloro-2/3-hydroxybenzaldehyde
	18.28	$[M]^+$ = 142,107,79,77,51 (C) 4-chlorobenzyl alcohol
	19.39	$[M]^+$ = 158,125,89,63,45 (D) 4-chlorobenzyl mercaptan
	31.48	$[M]^+$ = 229,158,125,89,72 (E) S-4-chlorobenzyl ethylthiocarbamate
	33.92	$[M]^+$ = 257, 125,100,72,44,29 (TBC) S-4-chlorobenzyl diethylthiocarbamate
	36.26	$[M]^+$ = 271,156,146,125,89,43 (F) S-4-chlorobenzyl acetyl(ethyl)thiocarbamate
	41.15	$[M]^+$ = 273,141,100,72,44,29 (G) S-4-chloro-2/3-hydroxybenzyl diethylthiocarbamate

Accordingly, pH 6 (also close to the initial pH of the mixture) was used in the following experiments.

3.2.4. Effects of anions on the degradation of TBC

The study of the effects of anions on the photocatalytic degradation of TBC was important because anions were rather common in natural water and industrial wastewater. The effects of the presence of various anions such as chloride, bicarbonate, carbonate, and sulfate were studied using 0.05 M solutions of their sodium salts and an initial concentration of 5 mg L⁻¹ of TBC with a 1 g L⁻¹ of BiVO₄ and 87.5 mg L⁻¹ of H₂O₂. The results showed that all these anions inhibited the degradation significantly (see Fig. 8). Inhibition effects of anions could be explained as the reaction of positive holes (h⁺) and hydroxyl radicals (HO·) with anions that behaved as h⁺ and HO· scavengers resulting in prolonged TBC removal [38]. A major drawback resulting from the high reactivity and non-selectivity of HO· was that it also reacted with non-target compounds present in the background water matrix, i.e. inorganic anions present in water. This result in a higher HO· demanded to accomplish the desired degree of degradation [39].

3.2.5. Performance of recycled catalyst

The stability and reusability of catalysts are very important issues for practical applications. To confirm the stability of the high photocatalytic performance of BiVO₄, the circulating runs in the photocatalytic degradation of thiobencarb in Vis/BiVO₄/H₂O₂

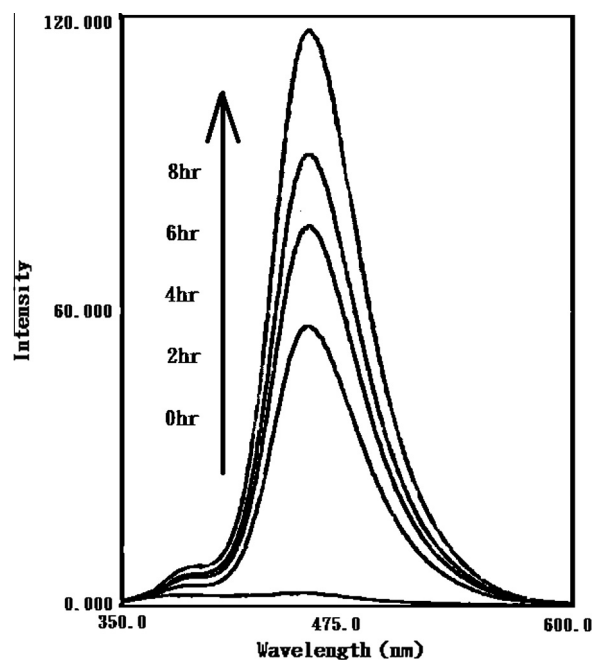


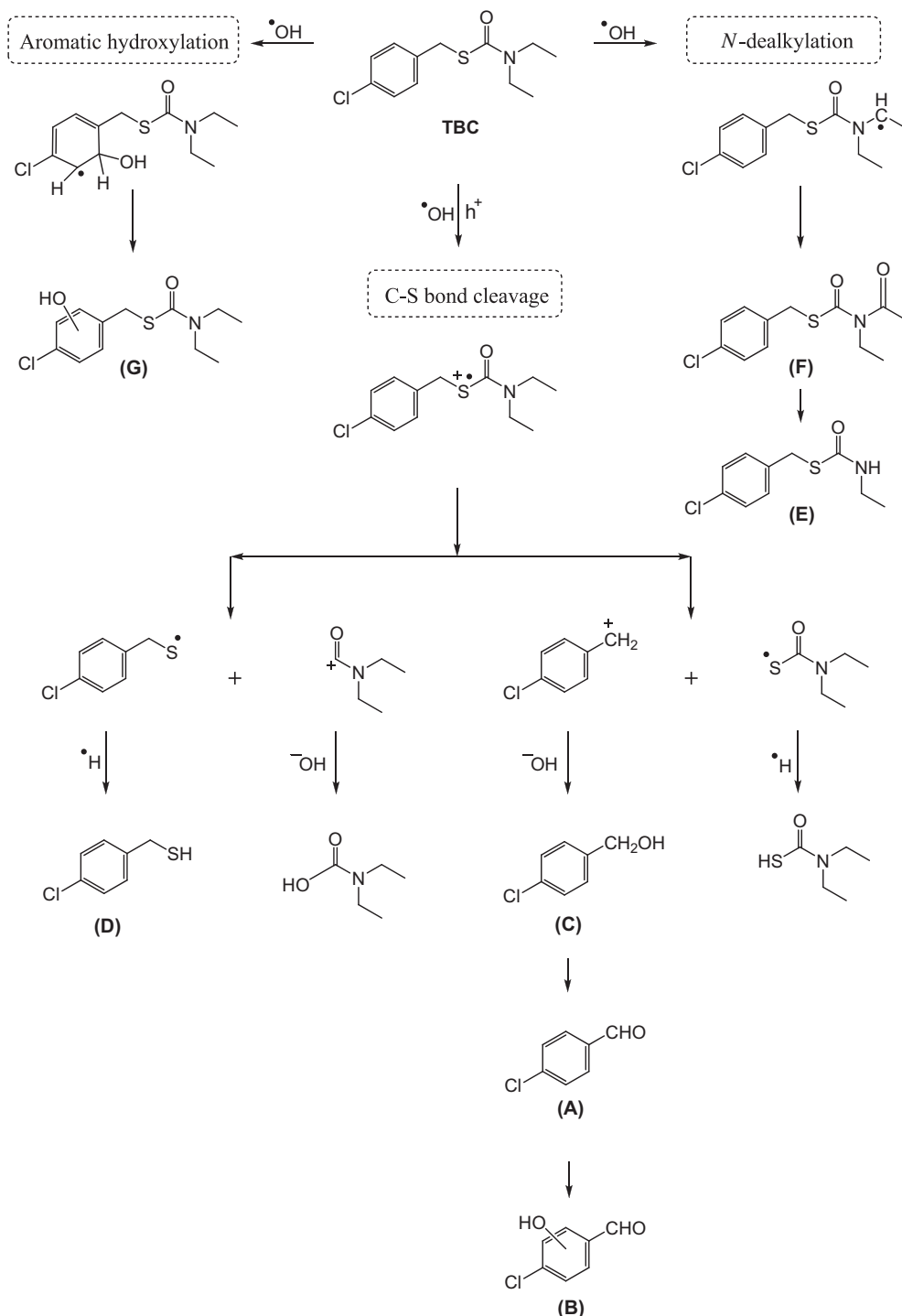
Fig. 11. Fluorescence spectral changes observed during illumination of BiVO₄/H₂O₂ in a 1 × 10⁻³ M aqueous solution of coumarin (excitation at 332 nm). Each fluorescence spectrum was recorded every 2 h of visible-light irradiation.

system was performed (Fig. 9). It could be seen that the catalyst did not exhibit a significant loss of activity in three successive runs. TBC removal remained higher than 97% in each cycle, confirming that BiVO_4 was not photocorroded and rather stable during the photocatalytic oxidation of TBC.

3.2.6. Separation and identification of the intermediates

In photocatalytic degradation process, the concentration of reaction intermediates was low and thus the intermediates had to be pre-concentrated before the application of an appropriate analytical procedure. Prior to GC/MS analysis, the samples were pre-concentrated using a solid-phase microextraction (SPME)

method, a selective tool for the trace analysis of organic compound in water samples. Therefore, the intermediates generated in the TBC solution during the photocatalytic degradation process with visible-light irradiation were examined with SPME-GC/MS. Fig. 10 displays the chromatogram of the TBC solution (100 mg L^{-1}) after irradiation for 14 h in the presence of BiVO_4 and H_2O_2 . At least eight compounds were identified at the retention time less than 45 min. One of the peaks was the initial TBC; the other seven (new) peaks were the intermediates formed. We denoted the related intermediates as compounds A–G. Except for the initial TBC, the other peaks increased at first and subsequently decreased, indicating formation and subsequent transformation of the



Scheme 1. Proposed photodegradation pathway of thiobencarb in the $\text{Vis}/\text{BiVO}_4/\text{H}_2\text{O}_2$ system.

intermediates. Some other minor peaks were present, but mass fragment information did not allow elucidation of their structures.

Table 1 summarizes the identified intermediates of TBC along with their retention time and the characteristic ions of the mass spectra. Four intermediates (compounds **A–D**) were identified by the molecular ion and mass fragment ions and also through the comparison with NIST library data. The similarities of these compounds to the NIST library data were more than 74%. Three intermediates (compounds **E–G**) not being included in the library were identified by the molecular ion and the interpretation of the mass spectra. The molecular mass of these intermediates was determined using positive ion chemical ionization (CI) mass spectrometry through the abundant protonated molecules, and then structural data were obtained from the electron impact (EI) fragmentation patterns. The presence and number of chlorine atoms in the suspected intermediates could be easily attained by taking into account both the relative intensity of the $^{35}\text{Cl}/^{37}\text{Cl}$ signals and the mass differences between the two masses. The detailed information for the intermediate identification was described in the [Supplementary data](#).

3.2.7. Degradation pathways of TBC

To understand the active species involved in the photocatalytic process, hydroxyl radicals ($\cdot\text{OH}$) were detected in the $\text{Vis}/\text{BiVO}_4/\text{H}_2\text{O}_2$ system by the fluorescence technique using coumarin as a probe molecule. Coumarin readily reacts with $\cdot\text{OH}$ to produce a highly fluorescent product, 7-hydroxycoumarin [40–42]. Fig. 11 shows the changes of fluorescence spectra from 10^{-3} M coumarin solution under visible-light irradiation with irradiation time in the presence of $\text{BiVO}_4/\text{H}_2\text{O}_2$. It could be seen that a gradual increase in the fluorescence intensity at about 456 nm was observed with increasing irradiation time. The generated fluorescence spectrum had the identical shape and maximum wavelength with that of standard 7-hydroxycoumarin. This suggested that fluorescent product 7-hydroxycoumarin was formed during BiVO_4 photocatalysis due to the specific reaction between $\cdot\text{OH}$ and coumarin. Therefore, hydroxyl radicals were shown to be the active species during BiVO_4 photocatalytic reaction.

Scheme 1 shows the proposed mechanism for the generation of the primary detected intermediates, which involved three different pathways, corresponding to the three possible reaction sites on the TBC molecule. One was based on the initial attack of the aromatic ring by $\text{HO}\cdot$ leading to the formation of hydroxylated derivative. The second route was based on the abstraction of hydrogen atoms of the *N*-alkyl group followed by the addition of oxygen resulting in dealkylated derivative. Finally, the third possible degradation route was based on the oxidative cleavage of the C–S bond of the substrate molecule.

Aromatic hydroxylation was a typical reaction of hydroxyl free radicals ($\text{HO}\cdot$) and involved hydroxycyclohexadienyl radical intermediates that were oxidized by molecular oxygen to the phenolic products [43]. Hydroxyl radicals attacked preferentially the aromatic moiety due to their electrophilic character to form the ring-hydroxylated product (compound **G**) but also attacked the *N*-alkyl chain to form the de-alkylated product (compound **E**). It was well known that the $\text{HO}\cdot$ radical was an electrophile and that C–H bonds adjacent to nitrogen were responsible for a pronounced stereoelectronic effect that produced high rates of H-atom abstraction. Therefore, the α -hydrogen atoms in the *N*-ethyl group of TBC molecule were the most prone to radical attack. Hydroxyl radicals yielded carbon-centered radicals upon the H-atom abstraction from the *N*-ethyl group, or they reacted with the lone-pair electron on the N atom to generate cationic radicals, which subsequently converted into carbon-centered radicals [44]. The carbon-centered radical generated after the addition of oxygen forming the peroxy

radical decomposed to different intermediates (compounds **E** and **F**).

In addition to the degradation routes of hydroxylation and *N*-de-ethylation, an alternative pathway was also identified. First, oxidation of the thiobencarb molecule to form the thiobencarb cation radical took place when positive holes attacked it, initiating a series of reactions. The formation of cation radicals had also been observed in the photocatalytic degradation of organophosphorus pesticides [45] and thioethers [46].

The interfacial transfer of a single electron from the sulfur atom led to the formation of thiobencarb cation radical. The scission of the C–S bond in this cation radical led to the formation of a $\text{ClC}_6\text{H}_4\text{-CH}_2\text{S}\cdot$ radical that was the precursor of 4-chlorobenzyl mercaptan (compound **D**). The H atom necessary for S–H bond formation was proposed to originate from the proton reduction by photogenerated electron $\text{H}^+ + \text{e}^- \rightarrow \text{H}\cdot$ as already observed in the degradation of the insecticide fenitrothion by Kerzhentsev et al. [47]. Similarly, the scission of the C–S bond in the TBC cation radical led to the formation of (4-chlorophenyl)methyl cation. The carbocation was extremely unstable and underwent rapid hydrolysis. Hydrolysis of (4-chlorophenyl)methyl cation yielded 4-chlorobenzyl alcohol (compound **C**). Subsequently, 4-chlorobenzyl alcohol underwent oxidation to 4-chlorobenzaldehyde (compound **A**) and 4-chloro-2/3-hydroxybenzaldehyde (compound **B**).

4. Conclusions

BiVO_4 photocatalyst with high crystallinity was successfully synthesized via an aqueous process. The structural studies revealed that the BiVO_4 powder exhibited the typical pattern for monoclinic scheelite structure. Thiobencarb could be successfully degraded in the $\text{Vis}/\text{BiVO}_4/\text{H}_2\text{O}_2$ system. At optimal operating parameters, its degradation efficiency could reach 97% in 5 h. After three recycles, the BiVO_4 catalyst did not exhibit any significant loss of photocatalytic activity, confirming the photocatalyst being essentially stable. The photocatalytic performance for TBC degradation was much enhanced with the assistance of appropriate amount of H_2O_2 . The photodegradation rate was found to increase with increasing BiVO_4 dosages, but the reaction was slower at high dosages. The thiobencarb degradation was much more efficient under acidic condition and decreased drastically with increasing pH. In addition, the presence of inorganic ions such as chloride, bicarbonate, carbonate, and sulfate, which were often present in natural water and industrial wastewater, decreased the photocatalytic degradation rate of TBC. Seven intermediates were identified and characterized through a mass spectra analysis, giving insight into the early steps of the degradation process. Results suggest that possible transformation pathways may include hydroxylation, dealkylation and C–S bond cleavage. This study not only provides useful information for the research of thiocarbamate decomposition, but also facilitates the development of new application of BiVO_4 .

Acknowledgment

This research was supported by the National Science Council of the Republic of China (NSC 101-2113-M-025-001).

Appendix A. Supplementary material

Supplementary data associated with this article can be found, in the online version, at <http://dx.doi.org/10.1016/j.seppur.2013.10.049>.

References

- [1] S.N. Pentylala, C.S. Chetty, Comparative studies on the changes in AChE and ATPase activities in neonate and adult rat brains under thiobencarb stress, *J. Appl. Toxicol.* 13 (1993) 39–42.
- [2] H. Jinno, N. Hanioka, A. Takahashi, T. Nishimura, T. Toyooka, M. Ando, Comparative cytotoxicity of the aqueous chlorination products of thiobencarb, a thiocarbamate herbicide, in cultured rat hepatocytes, *Toxicol. In Vitro* 11 (1997) 731–739.
- [3] S. Kodama, A. Yamamoto, A. Matsunaga, S-oxygenation of thiobencarb in tap water processed by chlorination, *J. Agric. Food Chem.* 45 (1997) 990–994.
- [4] Md.N. Amin, S. Kaneco, T. Kato, H. Katsumata, T. Suzuki, K. Ohta, Removal of thiobencarb in aqueous solution by zero valent iron, *Chemosphere* 70 (2008) 511–515.
- [5] S.H. Lin, R.S. Juang, Adsorption of phenol and its derivatives from water using synthetic resins and low-cost natural adsorbents: a review, *J. Environ. Manage.* 90 (2009) 1336–1349.
- [6] S. Wang, Y. Peng, Natural zeolites as effective adsorbents in water and wastewater treatment, *Chem. Eng. J.* 156 (2010) 11–24.
- [7] C.E. Schaefer, X. Yang, O. Pelz, D.T. Tsao, S.H. Stregger, R.J. Steffan, Aerobic biodegradation of iso-butanol and ethanol and their relative effects on BTEX biodegradation in aquifer materials, *Chemosphere* 81 (2010) 1104–1110.
- [8] A.K. Haritash, C.P. Kaushik, Biodegradation aspects of polycyclic aromatic hydrocarbons (PAHs): a review, *J. Hazard. Mater.* 169 (2009) 1–15.
- [9] T. Kadowaki, C.E. Wheelock, T. Adachi, T. Kudo, S. Okamoto, N. Tanaka, K. Tonomura, G. Tsujimoto, H. Mamitsuka, S. Goto, et al., Identification of endocrine disruptor biodegradation by integration of structure–activity relationship with pathway analysis, *Environ. Sci. Technol.* 41 (2007) 7997–8003.
- [10] M. Crimi, S. Ko, Control of manganese dioxide particles resulting from in situ chemical oxidation using permanganate, *Chemosphere* 74 (2009) 847–853.
- [11] K. Lin, W. Liu, J. Gan, Oxidative removal of bisphenol A by manganese dioxide: efficacy, products, and pathways, *Environ. Sci. Technol.* 43 (2009) 3860–3864.
- [12] C.C. Chen, R.J. Wu, I.C. Yao, C.S. Lu, Bis(2-chloroethoxy)methane degradation by TiO₂ photocatalysis: parameter and reaction pathway investigations, *J. Hazard. Mater.* 172 (2009) 1021–1032.
- [13] C.S. Lu, C.C. Chen, F.D. Mai, H.K. Li, Identification of the degradation pathways of alkanolamines with TiO₂ photocatalysis, *J. Hazard. Mater.* 165 (2009) 306–316.
- [14] H.F. Lai, C.C. Chen, R.J. Wu, C.S. Lu, Thiobencarb degradation by TiO₂ photocatalysis: parameter and reaction pathway investigations, *J. Chin. Chem. Soc.* 59 (2012) 87–97.
- [15] M. Sturini, E. Fasani, C. Prandi, A. Casaschi, A. Albin, Titanium dioxide-photocatalysed decomposition of some thiocarbamates in water, *J. Photochem. Photobiol. A: Chem.* 101 (1996) 251–255.
- [16] C.Y. Wang, H. Zhang, F. Li, L.Y. Zhu, Degradation and mineralization of bisphenol A by mesoporous Bi₂WO₆ under simulated solar light irradiation, *Environ. Sci. Technol.* 44 (2010) 6843–6848.
- [17] M. Shang, W. Wang, L. Zhou, S. Sun, W. Yin, Nanosized BiVO₄ with high visible-light-induced photocatalytic activity: ultrasonic-assisted synthesis and protective effect of surfactant, *J. Hazard. Mater.* 172 (2009) 338–344.
- [18] W. Yin, W. Wang, L. Zhou, S. Sun, L. Zhang, CTAB-assisted synthesis of monoclinic BiVO₄ photocatalyst and its highly efficient degradation of organic dye under visible-light irradiation, *J. Hazard. Mater.* 173 (2010) 194–199.
- [19] Y.K. Kho, W.Y. Teoh, A. Iwase, L. Madler, A. Kudo, R. Amal, Flame preparation of visible-light-responsive BiVO₄ oxygen evolution photocatalysts with subsequent activation via aqueous route, *ACS Appl. Mater. Interfaces* 3 (2011) 1997–2004.
- [20] A.M. Cruz, U.M.G. Perez, Photocatalytic properties of BiVO₄ prepared by the co-precipitation method: degradation of rhodamine B and possible reaction mechanisms under visible irradiation, *Mater. Res. Bull.* 45 (2010) 135–141.
- [21] J. Yu, Y. Zhang, A. Kudo, Synthesis and photocatalytic performances of BiVO₄ by ammonia co-precipitation process, *J. Solid State Chem.* 182 (2009) 223–228.
- [22] B. Xie, H. Zhang, P. Cai, R. Qiu, Y. Xiong, Simultaneous photocatalytic reduction of Cr(VI) and oxidation of phenol over monoclinic BiVO₄ under visible light irradiation, *Chemosphere* 63 (2006) 956–963.
- [23] B. Xie, C. He, P. Cai, Y. Xiong, Preparation of monoclinic BiVO₄ thin film by citrate route for photocatalytic application under visible light, *Thin Solid Films* 518 (2010) 1958–1961.
- [24] M. Shang, W. Wang, S. Sun, J. Ren, L. Zhou, L. Zhang, Efficient visible light-induced photocatalytic degradation of contaminant by spindle-like PANI/BiVO₄, *J. Phys. Chem. C* 113 (2009) 20228–20233.
- [25] S. Kohtani, M. Tomohiro, K. Tokumura, R. Nakagaki, Photooxidation reactions of polycyclic aromatic hydrocarbons over pure and Ag-loaded BiVO₄ photocatalysts, *Appl. Catal. B: Environ.* 58 (2005) 265–272.
- [26] S. Sun, W. Wang, L. Zhou, H. Xu, Efficient methylene blue removal over hydrothermally synthesized starlike BiVO₄, *Ind. Eng. Chem. Res.* 48 (2009) 1735–1739.
- [27] S. Kohtani, S. Makino, A. Kudo, K. Tokumura, Y. Ishigaki, T. Matsunaga, O. Nikaido, K. Hayakawa, R. Nakagaki, Photocatalytic degradation of 4-n-nonylphenol under irradiation from solar simulator: comparison between BiVO₄ and TiO₂ photocatalysts, *Chem. Lett.* 31 (2002) 660–661.
- [28] C.C. Chen, C.S. Lu, F.D. Mai, C.S. Weng, Photooxidative N-de-ethylation of anionic triarylmethane dye (sulfan blue) in titanium dioxide dispersions under UV irradiation, *J. Hazard. Mater.* B137 (2006) 1600–1607.
- [29] J. Tang, Z. Zou, J. Ye, Efficient photocatalytic decomposition of organic contaminants over CaBi₂O₄ under visible-light irradiation, *Angew. Chem. Int. Ed.* 43 (2004) 4463–4466.
- [30] Z. Zhang, W. Wang, M. Shang, W. Yin, Photocatalytic degradation of rhodamine B and phenol by solution combustion synthesized BiVO₄ photocatalyst, *Catal. Commun.* 11 (2010) 982–986.
- [31] L. Ge, Novel Pd/BiVO₄ composite photocatalysts for efficient degradation of methyl orange under visible light irradiation, *Mater. Chem. Phys.* 107 (2008) 465–470.
- [32] R. Maciel, G.L. Sant'Anna Jr., M. Dezotti, Phenol removal from high salinity effluents using Fenton's reagent and photo-Fenton reactions, *Chemosphere* 57 (2004) 711–719.
- [33] Q. Xiao, J. Zhang, C. Xiao, X.K. Tan, Photocatalytic degradation of methylene blue over Co₃O₄/Bi₂WO₆ composite under visible light irradiation, *Catal. Commun.* 9 (2008) 1247–1253.
- [34] J. Yu, L. Zhang, B. Cheng, Y. Su, Hydrothermal preparation and photocatalytic activity of hierarchically sponge-like macro-/mesoporous titania, *J. Phys. Chem. C* 111 (2007) 10582–10589.
- [35] J. Yu, X. Zhao, Q. Zhao, Effect of surface structure on photocatalytic activity of TiO₂ thin films prepared by sol–gel method, *Thin Solid Films* 379 (2000) 7–14.
- [36] W. Chu, W.K. Choy, T.Y. So, The effect of solution pH and peroxide in the TiO₂-induced photocatalysis of chlorinated aniline, *J. Hazard. Mater.* 141 (2007) 86–91.
- [37] C.Y. Chan, S. Tao, R. Dawson, P.K. Wong, Treatment of atrazine by integrating photocatalytic and biological processes, *Environ. Pollut.* 131 (2004) 45–54.
- [38] N.M. Mahmoodi, M. Arami, N.Y. Limaee, K. Gharanjig, Photocatalytic degradation of agricultural N-heterocyclic organic pollutants using immobilized nanoparticles of titania, *J. Hazard. Mater.* 145 (2007) 65–71.
- [39] I.K. Konstantinou, T.A. Albanis, TiO₂-assisted photocatalytic degradation of azo dyes in aqueous solution: kinetic and mechanistic investigations, a review, *Appl. Catal. B: Environ.* 49 (2004) 1–14.
- [40] Q. Xiang, J. Yu, P.K. Wong, Quantitative characterization of hydroxyl radicals produced by various photocatalysts, *J. Colloid Interface Sci.* 357 (2011) 163–167.
- [41] K. Ishibashi, A. Fujishima, T. Watanabe, K. Hashimoto, Detection of active oxidative species in TiO₂ photocatalysis using the fluorescence technique, *Electrochem. Commun.* 2 (2000) 207–210.
- [42] X. Yu, J. Yu, B. Cheng, B. Huang, One-pot template-free synthesis of monodisperse zinc sulfide hollow spheres and their photocatalytic properties, *Chem. Eur. J.* 15 (2009) 6731–6739.
- [43] W.M. Draper, D.G. Crosby, Photochemistry and volatility of drepamon in water, *J. Agric. Food Chem.* 32 (1984) 728–733.
- [44] J. Lee, W. Choi, Effect of platinum deposits on TiO₂ on the anoxic photocatalytic degradation pathways of alkylamines in water: dealkylation and N-alkylation, *Environ. Sci. Technol.* 38 (2004) 4026–4033.
- [45] E. Evgenidou, I. Konstantinou, K. Fytianos, T. Albanis, Study of the removal of dichlorvos and dimethoate in a titanium dioxide mediated photocatalytic process through the examination of intermediates and the reaction mechanism, *J. Hazard. Mater.* B137 (2006) 1056–1064.
- [46] M.A. Fox, A.A. Abdel-Wahad, Selectivity in the TiO₂-mediated photocatalytic oxidation of thioethers, *Tetrahedron Lett.* 31 (1990) 4533–4536.
- [47] M. Kerzhentsev, C. Guillard, J.-M. Herrmann, P. Pichat, Photocatalytic pollutant removal in water at room temperature: case study of the total degradation of the insecticide fenitrothion (phosphorothioic acid O, O-dimethyl-O-(3-methyl-4-nitro-phenyl) ester), *Catal. Today* 27 (1996) 215–220.